Constraints on multicomponent dark energy from cosmological observations

Ke Wang[1,2,*] and Lu Chen[3,†]

[1]*Lanzhou Center for Theoretical Physics, Key Laboratory of Theoretical Physics of Gansu Province,*
School of Physical Science and Technology, Lanzhou University,
Lanzhou 730000, People's Republic of China
[2]*Institute of Theoretical Physics and Research Center of Gravitation, Lanzhou University,*
Lanzhou 730000, People's Republic of China
[3]*School of Physics and Electronics, Shandong Normal University, Jinan 250014, China*

Dark energy (DE) plays an important role in the expansion history of our Universe. But we only got limited knowledge about its nature and properties after decades of study. In most numerical researches, DE is usually considered as a dynamical whole. Actually, multicomponent DE models can also explain the accelerating expansion of our Universe, which is accepted theoretically but lack numerical researches. We try to study the multicomponent DE models from observation by constructing w_nCDM models. The total energy density of DE is separated into n ($n = 2, 3, 5$) parts equally and every part has a constant equation of state w_i ($i = 1, 2...n$). We modify the Friedmann equation and the parametrized post-Friedmann description of DE, then put constraints on w_is from Planck 2018 TT, TE, EE + lowE + lensing, BAO data, and PANTHEON samples. The multicomponent DE models are favored if any w_nCDM model is preferred by observational data and there is no overlap between the highest and lowest values of w_is. We find the data combination supports the w_nCDM model when n is small and the w_2CDM model is slightly preferred by $\Delta\chi^2_{\min} = \Delta$Akaike information criterion(AIC) $= \Delta$Bayesian information criterion $= -2.48$ over the Chevallier-Polarski-Linder (CPL) model, but the largest value of w_i overlaps the smallest one. With larger n, the maximum and minimum of w_is do not overlap with each other, but $\chi^2_{\min}$ and AIC also increase. In brief, we find no obvious evidence that DE is composed of different components.

I. INTRODUCTION

The concept of dark energy (DE) has been widely accepted by many physicists since the discovery of cosmic accelerating expansion in 1998 [1,2]. Lots of methods have been proposed to study the properties of DE. The distance measurements are used to detect DE, such as the baryonic acoustic oscillation (BAO) observation [3–11] and surveys on Type Ia supernovae (SNIa) [12–14]. The formation of large scale structure [15–18] is also influenced by DE significantly due to its negative pressure. DE, as the largest proportion of the total energy density in today's Universe, also leaves footprints on the cosmic microwave background (CMB) [19–22]. However, the nature of DE is still a puzzle through decades of researches.

Theoretically, DE is considered as the cosmological constant first [23]. After that, fluids or fields, especially scalar fields [24–29], are also considered as candidates of DE. Numerically, DE is usually considered to be a cosmological constant or dynamical models with its equation of state (EOS) w that varies with redshift z. For the simple cases, w is constant -1 in the base ΛCDM model and it is a free parameter in the wCDM model. In the Chevallier-Polarski-Linder (CPL) model (also named the $w_0 w_a$CDM model) [30,31] and other dynamical DE models, w is assumed to be a function of z. They have been well investigated in previous works [21,22,32–35], both theoretically and numerically. In fact, there is another possibility that DE is composed of different components, such as multifield models [22,36–38]. Previous works indicate we cannot distinguish the multifield DE from a single-field DE unless perturbations are considered. DE perturbations can cluster and leave footprints on structure formation under some circumstances, which is the way we judge whether DE is a whole or not. However, there are few numerical works aiming to study the constitution of DE starting from observational data. In our work, we try to study models with multicomponent DE from cosmological observation. Assuming DE only has gravitational interaction or it is minimally coupled to other components of Universe, we

---
[*]wangkey@lzu.edu.cn
[†]Corresponding author.
chenlu@sdnu.edu.cn

023514-1

separate today's total DE energy density into n parts equally (hereafter w_nCDM model) and reconsider the cosmic expansion history, including the background and perturbation evolutions. Notice that "n parts" do not mean DE is composed of n kinds of candidates. Actually, it is just a numerical separation artificially. Then we denote the constant EOSs of different parts as w_is ($i = 1, 2 \ldots n$) and put constraints on them from observational data combination. We cannot tell the ith and the jth ($j = 1, 2 \ldots n, j \neq i$) parts belong to different components of DE if w_i and w_j overlap with each other conservatively. However, if any w_nCDM model satisfies both of the following conditions: (i) there is no overlap between the EOSs of any two parts at some confidence level and (ii) the model is favored by observational data, we will reach a conclusion that DE is composed of more than one candidate.

This paper is organized as follows. In Sec. II, we sketch out the background and perturbation evolutions of the w_nCDM models. We utilize the CMB data [22], BAO data [6–11], and SNIa measurement [14] to constrain different DE models and show our results in Sec. III. Finally, a brief summary is included in Sec. IV.

II. PARAMETRIZED POST-FRIEDMANN DESCRIPTION OF THE w_nCDM MODELS

In the w_nCDM models, we divide today's DE energy density into n parts equally. Then the total energy density of our Universe is

$$\rho_{\text{tot}}(a) = \rho_T(a) + \rho_{de}(a) = \rho_T(a) + \sum_{i=1}^{n} \rho_{de,i}(1)a^{-3-3w_i}. \tag{1}$$

Here $\rho_{de,i}(1)$ and w_i are today's energy density and the constant EOS of the ith DE part, respectively. ρ_{de} is the total DE energy density. The subscript T denotes all the other components excluding DE. $a = 1/(1 + z)$ is the scale factor. The Friedmann equation is modified with Eq. (1). Actually, considering only the background evolution, we can never distinguish a single-field DE from multifield DE because there always exists a single field leading to any observed Hubble parameter $H(z)$ [37]. But we still modify this part for safe and integrity.

Then the evolution of DE perturbation should be dealt with. To cross the phantom divide line, the evolution of DE perturbation is described with the parametrized post-Friedmann (PPF) description [39–43]. Note that we take phantom divide into account though current data do not support phantom divide crossing if they are used together [44]. There are three reasons for doing so: (i) the previous conclusion is acquired under the condition that DE is treated as a whole; (ii) some models of multicomponent DE with at least one noncanonical phantom component can explain phantom divide crossing at recent redshifts [45];

and (iii) there are uncertainties in numerical analysis with different data combinations. In the synchronous gauge, the perturbations of energy density and momentum of DE satisfy the following modified equations:

$$\rho_{de}\delta_{de} = -3\rho_{de}^{w}\frac{v_{de}}{k_H} - \frac{c_K k_H^2 H^2}{4\pi G}\Gamma, \tag{2}$$

$$\rho_{de}^{w}v_{de} = \rho_{de}^{w}v_T - \frac{k_H^2 H^2}{4\pi GF}\left[S - \Gamma - \frac{\dot{\Gamma}}{H}\right]. \tag{3}$$

Here ρ_{de}^{w} is defined as

$$\rho_{de}^{w} \equiv \sum_{i=1}^{n} \rho_{de,i}(1)a^{-3-3w_i}(1 + w_i). \tag{4}$$

$\delta_{de} = \delta\rho_{de}/\rho_{de} = \delta_{de,i} = \delta\rho_{de,i}/\rho_{de,i}$ is the density perturbation of total DE and $\delta\rho_{de} = \sum_{i=1}^{n}\delta\rho_{de,i}$. Note that it is reasonable to add them up directly if we assume different parts of DE are minimally coupled with each other in our models. v denotes velocity and $v_{de} = v_{de,i}$. G is Newton's constant. H is Hubble parameter. c_K is related to the background curvature of our Universe. For a spatial flat Universe, we have $c_K = 1$. $k_H = k/aH$, where k is the wave number in Fourier space. Overdot means the differentiation over cosmic time. Besides,

$$F = 1 + \frac{12\pi Ga^2}{k^2 c_K}(\rho_T + p_T), \tag{5}$$

$$S = \frac{4\pi G}{H^2}\frac{(v_T + k\alpha)}{k_H}\rho_{de}^{w}, \tag{6}$$

where $\alpha = a(\dot{h} + 6\dot{\eta})/2k^2$, and h and η are the metric perturbations in the synchronous gauge. PPF description provides a well approximation for minimally coupled scalar field DE models and many smooth DE models. Therefore, DE ought to be relatively smoother than matter inside a transition scale $c_s k_H = 1$,

$$\rho_{de}\delta_{de} \ll \rho_T\delta_T. \tag{7}$$

In order to satisfy this condition, we have the following differential equation for Γ:

$$(1 + c_\Gamma^2 k_H^2)\left[\Gamma + c_\Gamma^2 k_H^2\Gamma + \frac{\dot{\Gamma}}{H}\right] = S. \tag{8}$$

For any given evolution of Γ, there is a specific evolution of perturbations of DE. And $c_\Gamma = 0.4c_s$ for the evolution of scalar field models.

TABLE I. Constraints on the cosmological parameters in different DE models from the combination data of Planck 2018 TT, TE, EE + lowE + lensing, BAO data, and PANTHEON samples. The first set of error bars indicates the 68% limits and the second set in parentheses reflects the 95% limits. Note that we get their constraints with "action = 0" in CosmoMC packages, but we set "action=2" to get more accurate values of $\chi^2_{\min}$ and AIC.

	ΛCDM model	wCDM model	w_0w_aCDM model
$\Omega_b h^2$	$0.02243 \pm 0.00014(\pm0.00027)$	$0.02240 \pm 0.00014\binom{+0.00028}{-0.00027}$	$0.02238 \pm 0.00014(\pm0.00027)$
$\Omega_c h^2$	$0.1192 \pm 0.0009(\pm0.0017)$	$0.1196 \pm 0.0010\binom{+0.0020}{-0.0021}$	$0.1199 \pm 0.0011(\pm0.0021)$
$100\theta_{MC}$	$1.04101 \pm 0.00029\binom{+0.00056}{-0.00057}$	$1.04097 \pm 0.00029(\pm0.00059)$	$1.04092 \pm 0.00030(\pm0.00059)$
τ	$0.057^{+0.007}_{-0.008}\binom{+0.015}{-0.014}$	$0.055^{+0.007}_{-0.008}\binom{+0.015}{-0.014}$	$0.053 \pm 0.007(\pm0.015)$
$\ln(10^{10}A_s)$	$3.047^{+0.014}_{-0.015}\binom{+0.030}{-0.027}$	$3.045^{+0.014}_{-0.015}\binom{+0.029}{-0.027}$	$3.042 \pm 0.014\binom{+0.030}{-0.029}$
n_s	$0.9669^{+0.0036}_{-0.0035}\binom{+0.0069}{-0.0068}$	$0.9661 \pm 0.0038\binom{+0.0076}{-0.0075}$	$0.9653 \pm 0.0039\binom{+0.0078}{-0.0079}$
H_0 (km s^{-1} Mpc^{-1})	$67.71 \pm 0.40\binom{+0.78}{-0.77}$	$68.29 \pm 0.81\binom{+1.60}{-1.59}$	$68.23^{+0.81}_{-0.82}\binom{+1.62}{-1.61}$
$w(w_0)$	$\cdots$	$-1.0247^{+0.0313}_{-0.0316}(\pm0.0627)$	$-0.9507^{+0.0773}_{-0.0774}\binom{+0.1569}{-0.1531}$
w_a	$\cdots$	$\cdots$	$-0.3011^{+0.3165}_{-0.2743}\binom{+0.5781}{-0.5971}$
$\chi^2_{\min}$	3817.640	3817.106	3819.502
AIC	3829.640	3831.106	3835.502

	w_2CDM model	w_3CDM model	w_5CDM model
$\Omega_b h^2$	$0.02240 \pm 0.00014(\pm0.00027)$	$0.02241 \pm 0.00014(\pm0.00027)$	$0.02242 \pm 0.00014(\pm0.00027)$
$\Omega_c h^2$	$0.1195 \pm 0.0010(\pm0.0020)$	$0.1195 \pm 0.0010\binom{+0.0020}{-0.0021}$	$0.1194 \pm 0.0010(\pm0.0020)$
$100\theta_{MC}$	$1.04098 \pm 0.00030\binom{+0.00058}{-0.00059}$	$1.04098 \pm 0.00030(\pm0.00060)$	$1.04100^{+0.00030}_{-0.00029}(\pm0.00058)$
τ	$0.056^{+0.007}_{-0.008}\binom{+0.015}{-0.014}$	$0.056^{+0.007}_{-0.008}\binom{+0.015}{-0.014}$	$0.057^{+0.007}_{-0.008}\binom{+0.016}{-0.014}$
$\ln(10^{10}A_s)$	$3.046 \pm 0.014\binom{+0.029}{-0.027}$	$3.046 \pm 0.014\binom{+0.029}{-0.028}$	$3.048^{+0.014}_{-0.015}\binom{+0.030}{-0.028}$
n_s	$0.9661 \pm 0.0039\binom{+0.0077}{-0.0076}$	$0.9662 \pm 0.0039(\pm0.0076)$	$0.9666 \pm 0.0039\binom{+0.0077}{-0.0076}$
H_0 (km s^{-1} Mpc^{-1})	$68.30 \pm 0.80\binom{+1.60}{-1.56}$	$68.31^{+0.82}_{-0.81}\binom{+1.62}{-1.60}$	$68.49 \pm 0.82\binom{+1.65}{-1.60}$
w_1	$-0.9305^{+0.0612}_{-0.0787}\binom{+0.1327}{-0.1229}$	$-0.8600^{+0.0767}_{-0.0860}\binom{+0.1496}{-0.1430}$	$-0.7900^{+0.0780}_{-0.0771}\binom{+0.1498}{-0.1480}$
w_2	$-1.1592^{+0.1386}_{-0.0647}\binom{+0.1880}{-0.2361}$	$-1.0223^{+0.0896}_{-0.0874}\binom{+0.1629}{-0.1677}$	$-0.9192^{+0.0817}_{-0.0709}\binom{+0.1480}{-0.1512}$
w_3	$\cdots$	$-1.2356^{+0.1670}_{-0.0832}\binom{+0.2355}{-0.2857}$	$-1.0433^{+0.1020}_{-0.0760}\binom{+0.1720}{-0.1842}$
w_4	$\cdots$	$\cdots$	$-1.2097^{+0.1563}_{-0.0934}\binom{+0.2389}{-0.2714}$
w_5	$\cdots$	$\cdots$	$-1.5608^{+0.3731}_{-0.1446}\binom{+0.5252}{-0.6871}$
$\chi^2_{\min}$	3817.022	3816.911	3817.139
AIC	3833.022	3834.911	3839.139

III. RESULTS

We refer to CAMB + CosmoMC packages [46–48] and use the data combination of CMB, BAO, and SNIa measurements to constrain the EOSs of different DE models. Concretely, we use Planck2018 TT, TE.EE + lowE + lensing [22], the BAO measurements at $z = 0.122, 0.38, 0.51, 0.61, 0.81, 1.52, 2.34$ [6–10] (which are summarized in Ref. [11]), as well as the PANTHEON samples [14].

Based on the previous discussion in Sec. II, we divide today's total density of DE into $n = 2$, 3, or 5 parts averagely and modify both the background and perturbation evolutions of DE in each model. It is noted here we also modify the "halofit" code [49] included in CAMB package, which models the nonlinear matter power spectrum resulting from parametrized DE models. We run CosmoMC with "action = 0" to get the marginalized errors and "action = 2" to get the minimum values of χ^2. In

w_2CDM model, there are eight free parameters needed to be fitted: $\{\Omega_b h^2, \Omega_c h^2, 100\theta_{MC}, \tau, \ln(10^{10})A_s, n_s, w_1, dw_2\}$. In the case of w_3CDM model, dw_3 is added and there are nine free parameters. Another two free parameters $\{dw_4, dw_5\}$ are added in the w_5CDM model. Six of them are parameters in the base ΛCDM model. $\Omega_b h^2$ and $\Omega_c h^2$ are today's density of baryonic matter and cold dark matter, respectively, $100\theta_{MC}$ is 100 times the ratio of the angular diameter distance to the large scale structure sound horizon, τ is the optical depth, n_s is the scalar spectrum index, and A_s is the amplitude of the power spectrum of primordial curvature perturbations. w_1 is the largest one among all the values of w_i ($i = 1, 2...n$). dw_j ($j = 2$, 3, 4, 5) is the difference between the EOSs of two adjacent values. In other words, EOSs of different DE parts are listed from top to bottom as below: $w_1, w_2 = w_1 - dw_2, w_3 = w_1 - dw_2 - dw_3$, and so forth. The ranges of w_1 are set to be $[-10, 10]$ and
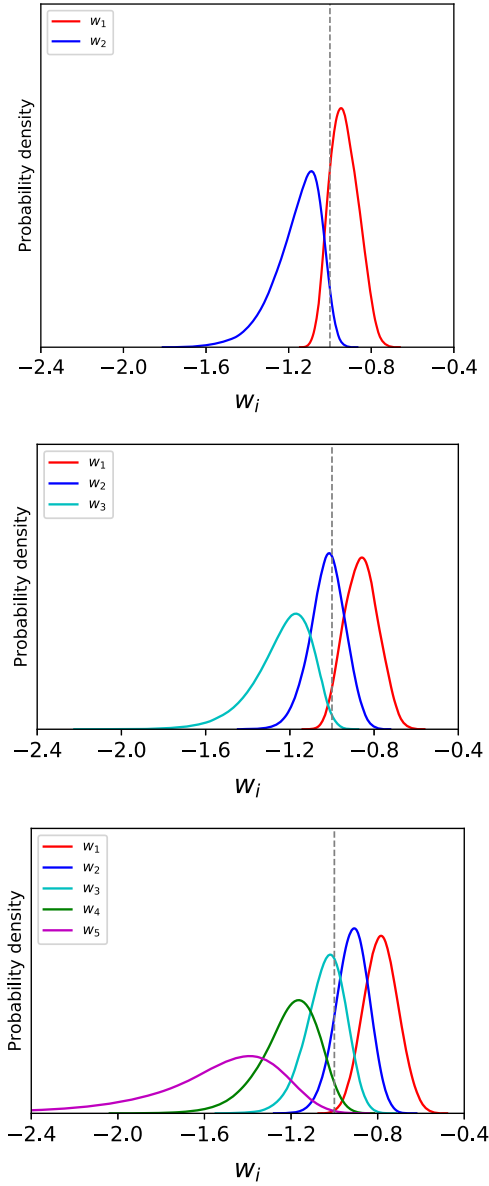
FIG. 1.   The probability densities of w_i ($i = 1, 2 \ldots n$) in the $w_n\text{CDM}$ ($n = 2, 3, 5$) model. From top to bottom are $w_2\text{CDM}$, $w_3\text{CDM}$, and $w_5\text{CDM}$ model. The gray dashed lines denote the phantom divide $w_i = -1$.

$dw_j \in [0, 3]$. For comparison, the ΛCDM, $w\text{CDM}$ and $w_0 w_a\text{CDM}$ models are also carried out.

The main results are shown in Table I. We show the 68% and 95% limits for the parameters in above six models. Besides, the probability densities of w_i in three $w_n\text{CDM}$ ($n = 2, 3, 5$) model are illustrated in Fig. 1 vividly. Notice that constraints on w_i are well around -1, but much weaker limits are acquired when w_i is much lower than -1 and there is a long left tail for w_n in the $w_n\text{CDM}$ model. This is because DE component with $w_i \ll -1$ has little influence on the relatively early Universe due to the suppression of scale factor in Eq. (1). Our constraints on the six parameters

of base ΛCDM model consist well with the values from Planck 2018 TT, TE, EE + lowE + lensing and BAO measurements given by Planck Collaboration [22]. In the $w_2\text{CDM}$ model, the highest value of EOSs is $w_1 = 0.9305^{+0.0612}_{-0.0787}$ at 68% C.L. and $w_1 = -0.9305^{+0.1327}_{-0.1229}$ at 95% C.L., while the lowest one is $w_2 = -1.1592^{+0.13886}_{-0.0647}$ at 68% C.L. and $-1.1592^{+0.1880}_{-0.2361}$ at 95% C.L. Although there is no overlap in the allowed ranges of 1σ, the overlap appears when their confidence level is around 2σ. We reach a similar conclusion in the $w_3\text{CDM}$ model. But it is not the case for the $w_5\text{CDM}$ model. We get the highest EOS as $w_1 = -0.7900^{+0.0780}_{-0.0771}$ at 68% C.L., $-0.7900^{+0.1498}_{-0.1480}$ at 95% C.L. and the lowest value as $w_5 = -1.5608^{+0.3731}_{-0.1446}$ at 68% C.L., $-1.5608^{+0.5252}_{-0.6871}$ at 95% C.L. It seems that the $w_5\text{CDM}$ model prefers multicomponent DE because w_1 and w_5 show no overlap with each other at 2σ. However, values of $\chi^2_{\min}$ and AIC are not conducive to $w_5\text{CDM}$ model. As Table I shows, we can sort these models by $\chi^2_{\min}$ from the smallest to the largest as $\{w_3\text{CDM}, w_2\text{CDM}, w\text{CDM}, w_5\text{CDM}, \Lambda\text{CDM}, w_0 w_a\text{CDM}\}$. Considering various numbers of free parameters in different models, we compare their Akaike information criterion (AIC) values with $\text{AIC} = \chi^2_{\min} + 2k$, where k is the number of free parameters [50–52]. So we put them in the order as $\{\Lambda\text{CDM}, w\text{CDM}, w_2\text{CDM}, w_3\text{CDM}, w_0 w_a\text{CDM}, w_5\text{CDM}\}$. However, the $w_3\text{CDM}$ and $w_5\text{CDM}$ models are extremely disfavored if we drop the AIC and use the Bayesian information criterion (BIC) given by $\text{BIC} = \chi^2_{\min} + k \ln N$ [53–56], where N denotes the number of data and has a very high value over 1000 in our work. The $w_2\text{CDM}$ model is preferred over the $w_0 w_a\text{CDM}$ model by $\Delta \chi^2_{\min} = \Delta\text{AIC} = \Delta\text{BIC} = -2.48$. All in all, none of the $w_n\text{CDM}$ ($n = 2, 3, 5$) models satisfies the two conditions in Sec. I. At this point, we find no obvious evidence of multicomponent DE.

Hereinafter, we focus on the $w\text{CDM}$, $w_0 w_a\text{CDM}$, and $w_2\text{CDM}$ models.

In Table I, values of Hubble constant H_0 are listed. In the $w_2\text{CDM}$ model, we have $H_0 = 68.30 \pm 0.80 \text{ km s}^{-1} \text{Mpc}^{-1}$ at 68% C.L. and $68.340^{+1.60}_{-1.56} \text{ km s}^{-1} \text{Mpc}^{-1}$ at 95% C.L., which are almost the same with values in the $w\text{CDM}$, $w_0 w_a\text{CDM}$ models and improves slightly over the ΛCDM model. Our results are consistent with Ref. [57], which reads $H_0 = 68.3^{+2.7}_{-2.6} \text{ km s}^{-1} \text{Mpc}^{-1}$ at 68% C.L. in the ΛCDM model and also in accord with some other H_0 estimates in Refs. [58–61]. They favor the Hubble constant from Planck Collaboration which is $H_0 = 67.4 \pm 0.5 \text{ km s}^{-1} \text{Mpc}^{-1}$ at 68% C.L. [22] and do not prefer $H_0 = 74.03 \pm 1.42 \text{ km s}^{-1} \text{Mpc}^{-1}$ from Hubble Space Telescope (HST) [62], as well as the results of Refs. [63–65]. These indicates that the $w_n\text{CDM}$ models are almost impossible to solve the Hubble tension between Planck and HST thoroughly. Moreover, we show the
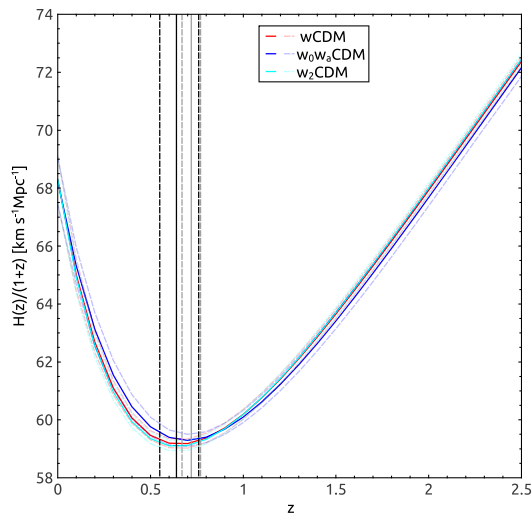
FIG. 2.   Comoving Hubble parameter $H(z)/(1+z)$ as a function of redshift z. The red, blue, and cyan lines represent $H(z)/(1+z)$ in the wCDM, w_0w_aCDM, and w_2CDM models, respectively. Their mean values and 68% limits are denoted with solid and dashed lines, respectively. Here the vertical black lines indicate the transition redshift $z_T = 0.64^{+0.12}_{-0.09}$ from combined data of SNIa, BAO, and cosmic chronometers (CC) data at low redshifts [66]. The vertical gray lines denote $z_T = 0.72 \pm 0.05$ from 38 measurements of $H(z)$ between redshifts $0.07 \leq z \leq 2.36$ [67].

comoving Hubble parameter $H(z)/(1+z)$ as a function of redshift z in Fig. 2. The evolution of $H(z)/(1+z)$ in the w_2CDM model is almost the same with that of the wCDM model. This is reasonable because w_1 and w_2 have a large overlap range in the w_2CDM model as shown in Fig. 1. And it has a slight difference from the w_0w_aCDM model.
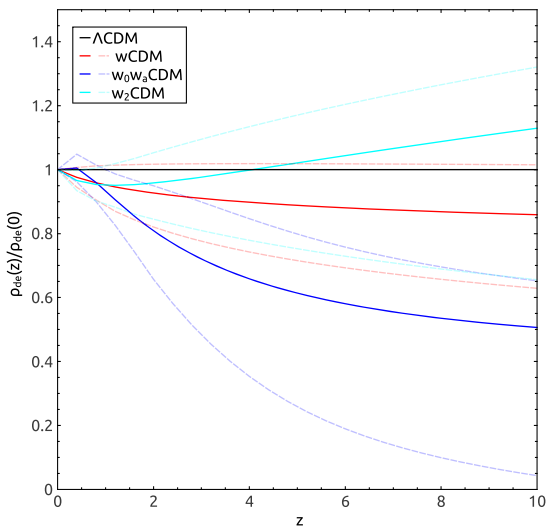

FIG. 3. $\rho_{de}(z)/\rho_{de}(0)$ as a function of redshift z. The horizontal black line with value of 1 indicates the values in the base ΛCDM model. The red and blue lines represent the values in the wCDM model and w_0w_aCDM model. The cyan lines denote those in the w_2CDM model. The dashed lines represent their upper and lower limits of 68% C.L.

The difference is too small to be observed. Thus, we cannot differentiate these models via the observable effects of $H(z)$. Figure 2 shows the onset of acceleration in the w_2CDM model is around $z_T = 0.6$, which is consistent with the result from Planck 2018 TT, TE, EE + lowE + lensing in the base ΛCDM model and Ref. [66]. We also show the other two transition redshifts estimated from different measurements: $z_T = 0.64^{+0.12}_{-0.09}$ from combined data of SNIa, BAO, and cosmic chronometers data at low redshifts [66]; $z_T = 0.72 \pm 0.05$ from 38 measurements of $H(z)$ between redshifts $0.07 \leq z \leq 2.36$ [67].

As shown in Fig. 3, we normalize $\rho_{de}(z)$ in the ΛCDM, wCDM, w_0w_aCDM, and w_2CDM models with their own $\rho_{de}(0)$. The parametrizations of wCDM model and w_0w_aCDM model provide almost monotonous DE density evolutions with redshift obviously. Contrastly, the lines cross over the standard line from bottom to top in the w_2CDM model. They have a ticklike density evolution. This means DE in the w_2CDM model can make a contribution to both late and early Universe. Thus, it is possible to differentiate the w_2CDM model from the wCDM model with other measurements.

IV. SUMMARY

In this paper, we try to investigate the multicomponent DE cosmological observations. New models named w_nCDM ($n = 2, 3, 5$) models are constructed assuming DE is composed of several equal parts with individual constant EOS w_i. The background and perturbation evolutions of DE are modified in the CAMB + CosmoMC packages. We also modify the "halofit" code included in the CAMB package because DE perturbations can cluster and influence the structure formation. Then we put constraints on parameters in the w_2CDM, w_3CDM, and w_5CDM models from Planck 2018 TT, TE, EE + lowE + lensing, BAO data, and PANTHEON samples. According to our results, the w_2CDM model is more favored over the w_0w_aCDM model and $\Delta\chi^2_{min} = \Delta AIC = \Delta BIC = -2.48$. The w_3CDM and w_5CDM models are disfavored due to their larger values of AIC or BIC. However, the allowed ranges of the highest values of w_is overlap with the lowest ones in the w_2CDM and w_3CDM models at about 2σ. When values of n get larger, the maximum and minimum of w_is in the w_nCDM models do not overlap, but the χ^2_{min}, AIC, and BIC also increase. In summary, we find no evidence of multicomponent DE in the w_nCDM ($n = 2, 3, 5$) models. Moreover, the w_2CDM and w_3CDM models fit observations better than the w_0w_aCDM model when χ^2_{min} and AIC are considered. We find an inspiration that the w_nCDM models may be better than the dynamical DE models with the same numbers of free parameters.

In addition, our results show that the transition redshift in the w_2CDM model is around $z \sim 0.6$ and the w_nCDM models can relieve the Hubble tension slightly, but cannot

solve it thoroughly. Besides, the plot of total DE energy density evolution indicates that the w_2CDM model has a ticklike density evolution which can make a contribution to both late and early Universe. So we can expect that experiments related to ρ_{de} will differentiate the w_2CDM and wCDM models.

[1] A. G. Riess *et al.* (Supernova Search Team), Astron. J. **116,** 1009 (1998).

[2] S. Perlmutter *et al.* (Supernova Cosmology Project), Astrophys. J. **517,** 565 (1999).

[3] S. Cole *et al.* (2dFGRS Collaboration), Mon. Not. R. Astron. Soc. **362,** 505 (2005).

[4] F. Beutler, C. Blake, M. Colless, D. Heath Jones, L. Staveley-Smith, L. Campbell, Q. Parker, W. Saunders, and F. Watson *et al.*, Mon. Not. R. Astron. Soc. **416,** 3017 (2011).

[5] A. J. Ross, L. Samushia, C. Howlett, W. J. Percival, A. Burden, and M. Manera, Mon. Not. R. Astron. Soc. **449,** 835 (2015).

[6] S. Alam *et al.* (BOSS Collaboration), Mon. Not. R. Astron. Soc. **470,** 2617 (2017).

[7] P. Carter, F. Beutler, W. J. Percival, C. Blake, J. Koda, and A. J. Ross, Mon. Not. R. Astron. Soc. **481,** 2371 (2018).

[8] T. M. C. Abbott *et al.* (DES Collaboration), Mon. Not. R. Astron. Soc. **483,** 4866 (2019).

[9] V. de Sainte Agathe, C. Balland, H. du Mas des Bourboux, N. G. Busca, M. Blomqvist, J. Guy, J. Rich, A. Font-Ribera, M. M. Pieri and J. E. Bautista *et al.*, Astron. Astrophys. **629,** A85 (2019).

[10] M. Ata *et al.*, Mon. Not. R. Astron. Soc. **473,** 4773 (2018).

[11] S. Cao, J. Ryan, and B. Ratra, Mon. Not. R. Astron. Soc. **497,** 3191 (2020).

[12] A. Conley *et al.* (SNLS Collaboration), Astrophys. J. Suppl. **192,** 1 (2011).

[13] N. Suzuki *et al.* (Supernova Cosmology Project), Astrophys. J. **746,** 85 (2012).

[14] D. M. Scolnic *et al.*, Astrophys. J. **859,** 101 (2018).

[15] A. Abate *et al.* (LSST Dark Energy Science Collaboration), arXiv:1211.0310.

[16] D. Alonso *et al.* (LSST Dark Energy Science Collaboration), arXiv:1809.01669.

[17] D. Korytov *et al.* (LSST Dark Energy Science Collaboration), Astrophys. J. Suppl. Ser. **245,** 26 (2019).

[18] M. Lochner *et al.* (LSST Dark Energy Science Collaboration), arXiv:1812.00515.

[19] E. Komatsu *et al.* (WMAP Collaboration), Astrophys. J. Suppl. Ser. **180,** 330 (2009).

[20] P. Ade *et al.* (Planck Collaboration), Astron. Astrophys. **571,** A16 (2014).

[21] P. Ade *et al.* (Planck Collaboration), Astron. Astrophys. **594,** A13 (2016).

[22] N. Aghanim *et al.* (Planck Collaboration), Astron. Astrophys. **641,** A6 (2020).

[23] P. Peebles and B. Ratra, Rev. Mod. Phys. **75,** 559 (2003).

[24] P. J. E. Peebles and B. Ratra, Astrophys. J. Lett. **325,** L17 (1988).

[25] B. Ratra and P. J. E. Peebles, Phys. Rev. D **37,** 3406 (1988).

[26] B. Novosyadlyj, O. Sergijenko, S. Apunevych, and V. Pelykh, Phys. Rev. D **82,** 103008 (2010).

[27] J. P. Johnson and S. Shankaranarayanan, Phys. Rev. D **103,** 023510 (2021).

[28] H. Mohseni Sadjadi, Phys. Dark Universe **30,** 100728 (2020).

[29] R. Kase and S. Tsujikawa, J. Cosmol. Astropart. Phys. 11 (2020) 032.

[30] E. V. Linder, Phys. Rev. Lett. **90,** 091301 (2003).

[31] M. Chevallier and D. Polarski, Int. J. Mod. Phys. D **10,** 213 (2001).

[32] S. Vagnozzi, S. Dhawan, M. Gerbino, K. Freese, A. Goobar, and O. Mena, Phys. Rev. D **98,** 083501 (2018).

[33] L. Chen, Q. G. Huang, and K. Wang, J. Cosmol. Astropart. Phys. 02 (2019) 028.

[34] L. Chen, Q. G. Huang, and K. Wang, Eur. Phys. J. C **77,** 762 (2017).

[35] Q. G. Huang, K. Wang, and S. Wang, J. Cosmol. Astropart. Phys. 12 (2015) 022.

[36] A. De Felice and S. Tsujikawa, Living Rev. Relativity **13,** 3 (2010).

[37] V. Vardanyan and L. Amendola, Phys. Rev. D **92,** 024009 (2015).

[38] Y. Akrami, M. Sasaki, A. R. Solomon, and V. Vardanyan, Phys. Lett. B **819,** 136427 (2021).

[39] W. Hu, Phys. Rev. D **77,** 103524 (2008).

[40] W. Fang, S. Wang, W. Hu, Z. Haiman, L. Hui, and M. May, Phys. Rev. D **78,** 103509 (2008).

[41] W. Fang, W. Hu, and A. Lewis, Phys. Rev. D **78,** 087303 (2008).

[42] J. Grande, A. Pelinson, and J. Sola, Phys. Rev. D **79,** 043006 (2009).

[43] Y. H. Li, S. Wang, X. D. Li, and X. Zhang, J. Cosmol. Astropart. Phys. 02 (2013) 033.

[44] C. G. Park and B. Ratra, Astrophys. Space Sci. **364,** 82 (2019).

[45] S. Nesseris and L. Perivolaropoulos, J. Cosmol. Astropart. Phys. 01 (2007) 018.

[46] A. Lewis, A. Challinor, and A. Lasenby, Astrophys. J. **538,** 473 (2000).

[47] A. Lewis and S. Bridle, Phys. Rev. D **66,** 103511 (2002).

[48] A. Lewis, Phys. Rev. D **87,** 103529 (2013).

[49] A. Mead, C. Heymans, L. Lombriser, J. Peacock, O. Steele, and H. Winther, Mon. Not. R. Astron. Soc. **459,** 1468 (2016).

[50] A. R. Liddle, Mon. Not. R. Astron. Soc.: Lett. **377,** L74 (2007).

[51] N. Sugiura, Commun. Stat., Theory Methods **7,** 13 (1978).

[52] Y. Gong and X. Chen, Phys. Rev. D **76,** 123007 (2007).

[53] G. Schwarz, Ann. Stat. **6,** 461 (1978).

[54] M. Biesiada, J. Cosmol. Astropart. Phys. 02 (2007) 003.

[55] A. Kurek and M. Szydlowski, Astrophys. J. **675,** 1 (2008).

[56] A. R. Liddle, Mon. Not. R. Astron. Soc. **351,** L49 (2004).

[57] Y. Chen, S. Kumar, and B. Ratra, Astrophys. J. **835,** 86 (2017).

[58] M. Rigault, G. Aldering, M. Kowalski, Y. Copin, P. Antilogus, C. Aragon, S. Bailey, C. Baltay, D. Baugh, and S. Bongard *et al.*, Astrophys. J. **802,** 20 (2015).

[59] K. Blum, E. Castorina, and M. Simonović, Astrophys. J. Lett. **892,** L27 (2020).

[60] W. L. Freedman, B. F. Madore, T. Hoyt, I. S. Jang, R. Beaton, M. G. Lee, A. Monson, J. Neeley, and J. Rich, arXiv:2002.01550.

[61] S. Birrer, A. J. Shajib, A. Galan, M. Millon, T. Treu, A. Agnello, M. Auger, G. C. F. Chen, L. Christensen, and T. Collett *et al.*, Astron. Astrophys. **643,** A165 (2020).

[62] A. G. Riess, S. Casertano, W. Yuan, L. M. Macri, and D. Scolnic, Astrophys. J. **876,** 85 (2019).

[63] B. R. Zhang, M. J. Childress, T. M. Davis, N. V. Karpenka, C. Lidman, B. P. Schmidt, and M. Smith, Mon. Not. R. Astron. Soc. **471,** 2254 (2017).

[64] S. Dhawan, S. W. Jha, and B. Leibundgut, Astron. Astrophys. **609,** A72 (2018).

[65] D. Fernández Arenas, E. Terlevich, R. Terlevich, J. Melnick, R. Chávez, F. Bresolin, E. Telles, M. Plionis, and S. Basilakos, Mon. Not. R. Astron. Soc. **474,** 1250 (2018).

[66] B. S. Haridasu, V. V. Luković, M. Moresco, and N. Vittorio, J. Cosmol. Astropart. Phys. 10 (2018) 015.

[67] O. Farooq, F. R. Madiyar, S. Crandall, and B. Ratra, Astrophys. J. **835,** 26 (2017).